CrossMark

Abiotic O_2 Levels on Planets around F, G, K, and M Stars: Effects of Lightning-produced Catalysts in Eliminating Oxygen False Positives

C. E. Harman[1,2,3] , R. Felton[4,5], R. Hu[6,7], S. D. Domagal-Goldman[3,5,8] , A. Segura[3,9], F. Tian[10] , and J. F. Kasting[11,12]

[1] Goddard Institute of Space Studies, 2880 Broadway, New York, NY 10027, USA; chester.e.harman@nasa.gov
[2] Department of Applied Physics and Applied Mathematics, Columbia University, 500 W. 120th St., Mudd 200, MC 4701 New York, NY 10027, USA
[3] NASA Astrobiology Institute—Virtual Planetary Laboratory, USA
[4] Department of Physics, Catholic University of America, 620 Michigan Ave., N.E., Washington, DC 20064, USA
[5] Sellers Exoplanet Environments Collaboration, USA
[6] Jet Propulsion Laboratory, California Institute of Technology, Pasadena, CA 91109, USA
[7] Division of Geological and Planetary Sciences, California Institute of Technology, Pasadena, CA 91125, USA
[8] Planetary Systems Laboratory, NASA Goddard Space Flight Center, 8800 Greenbelt Road, Greenbelt, MD 20771, USA
[9] Instituto de Ciencias Nucleares, Universidad Nacional Autonoma de Mexico, Circuito Interior S/N, C.U. A.P. 70-543, Mexico, DF 04530, Mexico
[10] Ministry of Education Key Laboratory for Earth System Modeling, Department of Earth System Science, Tsinghua University, Beijing 100084, People's Republic of China
[11] Department of Geosciences, Pennsylvania State University, University Park, PA 16802, USA
[12] Center for Exoplanets and Habitable Worlds, Pennsylvania State University, University Park, PA 16802, USA

Abstract

Over the last few years, a number of authors have suggested that, under certain circumstances, molecular oxygen (O_2) or ozone (O_3) generated by abiotic processes may accumulate to detectable concentrations in a habitable terrestrial planet's atmosphere, producing so-called "false positives" for life. But the models have occasionally disagreed with each other, with some predicting false positives, and some not, for the same apparent set of circumstances. We show here that photochemical false positives derive either from inconsistencies in the treatment of atmospheric and global redox balance or from the treatment (or lack thereof) of lightning. For habitable terrestrial planets with even trace amounts of atmospheric N_2, NO produced by lightning catalyzes the recombination of CO and O derived from CO_2 photolysis and should be sufficient to eliminate all reported false positives. Molecular oxygen thus remains a useful biosignature gas for Earth-like extrasolar planets, provided that the planet resides within the conventional liquid water habitable zone and has not experienced distinctly non-Earth-like, irrecoverable water loss.

Key words: planet–star interactions – planets and satellites: atmospheres – planets and satellites: composition – planets and satellites: terrestrial planets

1. Introduction

In our search for life on planets orbiting other stars, detection strategies most often focus on how life here on Earth has modified its environment. Over geological timescales, photosynthesis by cyanobacteria (and later, by algae and plants) has increased the atmospheric molecular oxygen (O_2) concentration from negligible values to 21% by volume today. The increase in O_2 is thought to have occurred mostly in two or three major steps. The first was the Great Oxidation Event (GOE) some 2.5 billion years ago (Gya); the second is sometimes called the Neoproterozoic Oxidation Event (NOE), which took place ∼0.8 Gya (Kump 2008; Lyons et al. 2014). A third major increase may have occurred at around 400 Ma during the late Devonian period (Wallace et al. 2017). Atmospheric O_2 may have climbed even higher (up to ∼35% by volume) during the Carboniferous (e.g., Berner & Canfield 1989; see also Lenton 2001), but this increase was not sustained. Oxygen would have been difficult to observe remotely at low spectral resolution prior to the GOE and should have been easily detectable following the NOE (Segura et al. 2003; Harman et al. 2015). Whether O_2 and its photochemical byproduct, ozone (O_3), were

remotely observable during the intervening Proterozoic Eon depends on how much of it was present at that time. Estimates for Proterozoic O_2 range from 0.5 PAL (times the present atmospheric level) (Kump 2008) to <0.1% PAL (Planavsky et al. 2014). Ozone may have been detectable throughout the Proterozoic, even at lower O_2 concentrations, due to its strong UV absorption features (Segura et al. 2003).

Whether oxygenic photosynthesis would evolve on another Earth-like planet is unknown. Some authors have argued that it is a natural consequence of the ready availability of liquid water (H_2O) and carbon dioxide (CO_2) (e.g., Kiang et al. 2007; Léger et al. 2011). If so, then photosynthetic O_2 could be common on terrestrial planets within the habitable zone (Kasting et al. 1993b; Kopparapu et al. 2013) of their parent star (Kiang et al. 2007; Léger et al. 2011; Meadows 2017). Molecular oxygen or ozone could thus be one of the first biosignature gases detected remotely using a next-generation space telescope like the *James Webb Space Telescope* (*JWST*) (Schwieterman et al. 2016). O_2 and O_3 satisfy both the survivability and detectability criteria for biosignature gases (Seager et al. 2013; Meadows 2017; Meadows et al. 2017). Whether they also satisfy the third necessary criterion, reliability, has been a topic of recent debate. Understanding their reliability is critical and urgent, as *JWST* will begin observations within the next two years, and the detection of O_2 and O_3 are also central to the design of instruments for other future ground- and space-based telescopes (Domagal-Goldman et al. 2014; Harman et al. 2015; Meadows 2017; Meadows et al. 2017). Here, we

argue that O_2 and O_3 *are* reliable bioindicators under certain conditions. We outline what those conditions are, and discuss the secondary measurements and constraints necessary to demonstrate the presence of such conditions on another world.

2. False Positives in the Literature

For the purposes of this paper, a "false positive" for life is defined as any abiotically derived O_2 concentration that exceeds that estimated to follow the GOE (Harman et al. 2015). If the low estimates by Planavsky et al. (2014) are correct, then that level is at or below 0.1% PAL. Possible mechanisms by which that abiotic O_2 level might be achieved have been recently reviewed by Meadows (2017) and Meadows et al. (2017). Broadly speaking, these scenarios can be divided into two categories: (1) false positives driven by changes in the redox budget of a planet's combined atmosphere/ocean system (as defined in Catling & Kasting 2017, Ch. 8), and (2) false positives driven by photochemistry within the atmosphere.

Examples of the redox-driven false positives include planets that experience substantial water loss because they are located inside the inner edge of the habitable zone (Kasting 1988; Kasting et al. 1993a), or their host (M) stars are relatively bright during their pre-main sequence lifetimes (Ramirez & Kaltenegger 2014; Luger & Barnes 2015; Tian 2015), or they lack non-condensable gases like N_2 that help keep water vapor contained in the lower atmosphere (Wordsworth & Pierrehumbert 2014). In each of these cases, hydrogen is irreversibly lost to space, oxidizing the atmosphere and oceans and, ultimately, the planet itself. The ultimate fate of this oxygen is uncertain but it could potentially be drawn down to undetectable concentrations by absorption into the mantle (Wordsworth et al. 2018). Other types of redox-driven false positives essentially correspond to hypothetical planetary scenarios that lack a volcanic source of reduced gases (e.g., Hu et al. 2012; Domagal-Goldman et al. 2014; Gao et al. 2015). If volcanic outgassing is assumed to be nearly zero, or the recombination of CO and O_2 is inefficient, or there are no surface sinks for O_2, then O_2 can build up in the atmosphere. If reduced volcanic gas emissions are entirely neglected, O_2 can and must accumulate as H_2O is photolyzed and the resulting hydrogen escapes to space. But we argue that a false positive driven by such low outgassing rates is unlikely if the planet is habitable, so that liquid water can facilitate reactions of O_2 with its crust, *and* if the planet remains volcanically active for long time periods, as the Earth has done. (We return to this last point in Section 6.)

The false positive scenario described by Hu et al. (2012) is more complicated in that it has balanced hydrogen escape with both surface deposition and volcanic emission. For a 90% CO_2, 10% N_2 atmosphere on an abiotic planet orbiting a G star, they predict an O_2 mixing ratio of 1.3×10^{-3}, or 0.006 PAL (see their Figure 6 and Table 7). This scenario has no H_2 outgassing but a finite source of volcanic H_2S. The H_2S source exceeds the rate of hydrogen escape to space (after stoichiometric weighting to put these fluxes in the same redox units). Hence, the scenario has the excess hydrogen balanced by deposition of reduced species to the surface. As such, the redox budget of the ocean is unbalanced. This is equivalent to assuming production and burial of organic carbon on a planet that has no biological means of producing it. We have simulated additional scenarios (not shown) using the same model as Hu et al. (2012). For one scenario, we remove the previously assumed volcanic outgassing of H_2S, and for the other we remove both the H_2S

source and hydrogen escape. These two additional scenarios produce similar O_2 and O_3 mixing ratio profiles to that in Hu et al. (2012), and they both balance global redox. Importantly, all of the scenarios discussed in this paragraph allow O_3 to be deposited at the surface, but not O_2. This contributes to the buildup of atmospheric O_2, but it is not a physically realistic assumption, as reduced species (e.g., dissolved ferrous iron) should react with both. The assumption of zero volcanic outgassing of reduced gases is also not geologically plausible for an Earth-like planet, as rocky planetary interiors are expected to be generally reduced and as volcanism is difficult to suppress entirely on a planet as large as Earth. To put this another way, the presence or absence of a false positive for Earth-like planets around Sun-like stars is sensitive to the boundary conditions but, ultimately, the choice of boundary conditions must reflect a geologically plausible case.

Most of the redox-driven false positives should be identifiable remotely, given enough observations. Runaway greenhouse planets like early Venus would be suspect because of their position near or inside the inner edge of the habitable zone (Kasting 1988; Kopparapu et al. 2013; Kane et al. 2014; Way et al. 2016). Planets around late M stars should all be initially suspect, for the reasons just mentioned. One would need to verify that they have retained some of their water, potentially through spectral observations of the strong water vapor absorption feature at $\sim$0.95 μm, before assigning any significance to observed O_2 or O_3. Planets with very low N_2 ($<$0.5 bar) could, in principle, be identified by the absence of absorption by the N_2 dimer, by decreased Rayleigh scattering, or by sufficiently detailed spectra to show the effect of pressure on other absorption features (Schwieterman et al. 2015). The total pressure for the Archean atmosphere may have been $<$0.5 bar (Som et al. 2012, 2016), suggesting that N_2 would have been largely undetectable during this interval. Methods for identifying these false positive-generating mechanisms have been extensively discussed in the recent literature (Harman et al. 2015; Meadows 2017; Meadows et al. 2017).

The second category of false positives, those caused by photochemical processes, are more difficult to rule out, as these can ostensibly occur on worlds nearly indistinguishable from modern or ancient Earth. The case that we focus on here concerns planets around M dwarf host stars (Domagal-Goldman et al. 2014; Tian et al. 2014; Harman et al. 2015). This case is of great interest because *JWST* may be able to obtain transit spectra of such planets in the near future.
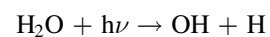
This particular photochemical false positive arises for the following reason. On Earth-like planets around *any* type of star, atmospheric CO_2 should be photolyzed by UV radiation shortward of 200 nm:

$$CO_2 + h\nu \rightarrow CO + O.$$
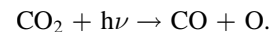
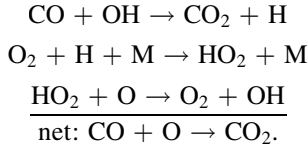The reaction between CO and O to reform CO_2 is spin-forbidden and slow, so the O atoms can recombine with each other to form O_2:

$$O + O + M \rightarrow O_2 + M.$$
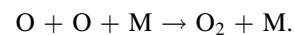
On planets like the early Earth, the rate of O_2 formation is relatively slow because CO and O can also recombine with each other by catalytic cycles involving the byproducts of water vapor photolysis:

$$H_2O + h\nu \rightarrow OH + H$$

followed by

$$CO + OH \rightarrow CO_2 + H$$
$$O_2 + H + M \rightarrow HO_2 + M$$
$$\underline{HO_2 + O \rightarrow O_2 + OH}$$
$$\text{net: } CO + O \rightarrow CO_2.$$

This sequence happens relatively quickly on early Earth because the Sun puts out plenty of near-UV radiation ($\lambda < 240$ nm) that can dissociate H_2O, as well as HO_2 and H_2O_2, thus initiating the cycle. But M stars are deficient in near-UV ($\sim$200–400 nm) radiation (e.g., Miles & Shkolnik 2017), so H_2O-, HO_2-, and H_2O_2-sourced catalytic cycles are much slower.

The potential for photochemical false positives on M-star planets has recently been studied by three different groups (Domagal-Goldman et al. 2014; Tian et al. 2014; Harman et al. 2015). Tian et al. and Harman et al. both found substantial false positives for such planets, i.e., surface abiotic O_2 concentrations that should be remotely detectable. For the same sets of conditions, Domagal-Goldman et al. found that only O_3 (and not O_2) accumulated to detectable levels. All three of these models were redox-balanced and should, in principle, have given similar results. (Indeed, all three models are derivatives of the same Kasting-group photochemical model.) The present study was motivated by the desire to figure out why they disagreed.

Having completed the analysis, we find that most of the differences between the Tian/Harman results and the Domagal-Goldman results were caused by the neglect of lightning in the first two models and its inclusion in the third, as well as methodological differences in addressing global redox. Lightning creates nitrogen oxides that can help catalyze the recombination of CO with O. Below, we briefly review how lightning affects planetary atmospheres in general, and then discuss its importance for the question of false positives on exoplanets.

3. Effect of Lightning on Atmospheric Photochemistry

3.1. Lightning Occurrence

The modern Earth experiences a global average of two to three lightning flashes $km^{-2}\,yr^{-1}$ ($\sim$2 $\times$ 10^{-4} flashes $km^{-2}\,hr^{-1}$), while the gas giants Jupiter and Saturn have lower lightning flash rates ($\sim$1–50 $\times$ 10^{-7} flashes $km^{-2}\,hr^{-1}$), and Venus has even fewer lightning flashes ($\sim$4 $\times$ 10^{-11} flashes $km^{-2}\,hr^{-1}$) (Hodosán et al. 2016 and references therein). Lightning on Earth is approximately an order of magnitude less frequent over oceans than over land (Hodosán et al. 2016), due to several potential contributing factors, including greater efficiency in converting the convective available potential energy (CAPE) into strong updrafts over land (e.g., Williams & Stanfill 2002). Lightning occurrence is a strong function of CAPE, so warmer, wetter atmospheres tend to produce more lightning (Wong et al. 2017). Additionally, some authors have suggested a connection between galactic cosmic rays (GCRs) and lightning (Stozhkov 2003 and references therein), which may enhance lightning for M dwarf planets experiencing higher GCR fluxes (Airapetian et al. 2017). We will return to GCRs briefly below.

3.2. Lightning Production of NO

On the modern Earth, lightning affects the chemical composition of the atmosphere by converting (or "fixing") N_2 and O_2 into
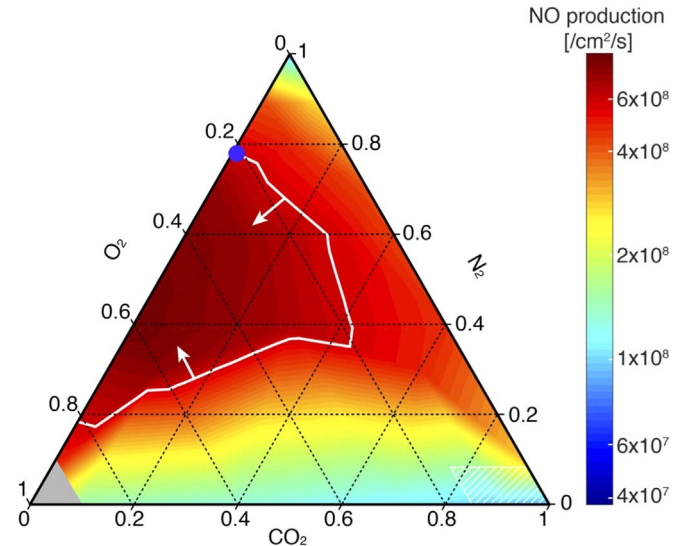
Figure 1. Lightning production of NO for a $CO_2/N_2/O_2$ atmosphere with $\sim$1% water vapor, where $f(CO_2)+f(N_2)+f(O_2) = 1$ (each as a fraction of the non-condensable component of the atmosphere). The white-hatched region at the bottom right corresponds to N_2 and O_2 concentrations at or below the level defined by Wordsworth & Pierrehumbert (2014) as being susceptible to abiotic O_2 accumulation from water loss. NO production in excess of modern ($>\sim$6 $\times$ 10^8 $cm^{-2}\,s^{-1}$) is highlighted by the white boundary, with arrows pointing toward higher NO production. For low concentrations of CO_2 and O_2 ($<$100 ppm), NO production is supported by oxygen derived from water vapor, remaining greater than $\sim$3 $\times$ 10^7 $cm^{-2}\,s^{-1}$ ($\sim$5% of modern); O_2 concentrations $>$0.9 bar (gray region) were not tested. The modern Earth's atmospheric composition is shown as the blue circle.

more reactive NO_x species, which can influence the concentrations of gases such as O_3 and OH (e.g., Chameides 1978). Given the high temperatures and pressures within the lightning flash, the equilibrium reactions can be written as

$$N_2 + O_2 \leftrightarrow 2NO$$
$$N_2 + 2H_2O \leftrightarrow 2NO + H_2$$
$$N_2 + 2CO_2 \leftrightarrow 2NO + 2CO.$$
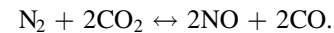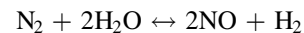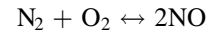
Thus, the oxygen used to form NO can be derived from CO_2, O_2, or water vapor. The ancient Earth would also have featured lightning-driven nitrogen fixation (Chameides & Walker 1981; Navarro-Gonzalez et al. 2001), with lower NO production compared to modern, as the early Earth's atmosphere is thought to have lacked significant amounts of O_2 (Kasting 1979). Other planets in our solar system, including Venus and Mars, could also have lightning-influenced chemistry (e.g., Nna Mvondo et al. 2001).

On Earth today, each lightning flash produces 30–670 moles of NO, with a typical lightning flash producing $\sim$250 moles of NO (Schumann & Huntrieser 2007). When integrated over the surface of the Earth, this yields a global NO production rate of $\sim$5 Tg yr^{-1}, or $\sim$6 $\times$ 10^8 NO molecules $cm^{-2}\,s^{-1}$ (Schumann & Huntrieser 2007). We use this as our estimate for the global lightning production of NO on the modern Earth. Figure 1 shows the production rate of NO from lightning in 1 bar, CO_2–O_2–N_2-dominated atmospheres, using a lightning parameterization updated from Kasting (1979) that assumes a freeze-out temperature of 3500 K for all constituents (Kasting 1990), which broadly agrees with other lightning simulations (e.g., Rimmer & Helling 2016). We have assumed the same surface temperature (288 K) for each composition, broadly

consistent with the presence of a carbonate–silicate feedback cycle that helps to stabilize a planet's climate (e.g., Kasting et al. 1993a; Kopparapu et al. 2013). This results in a water vapor mixing ratio of ∼1% at the surface.

We have chosen the ternary diagram in Figure 1 to highlight the dependence of NO production on composition, and we acknowledge that some of the mixtures represented may not correspond to physically self-consistent gas assemblages. That said, we note several effects. (1) NO production is highest for approximately present-day N_2 concentrations with higher-than-present-day O_2 concentrations. We have highlighted this region with a white boundary, with arrows pointing toward higher NO production. (2) NO production remains within an order of magnitude of modern NO production throughout the diagram, except at very low CO_2 and O_2 concentrations, where oxygen contributions to NO formation are sustained by water vapor in the atmosphere and where the "floor" is approximately 5% of modern NO fluxes (Kasting 1979). (3) At low N_2 concentrations (down to ∼1% N_2), NO production remains within a factor of 5 of the modern value. However, these low N_2 concentrations would likely result in abiotic accumulation of O_2 from water loss (Wordsworth & Pierrehumbert 2014)—a redox-based false positive. This region of parameter space is shown by the white-hatched area in the lower-right corner of the diagram. Taken together, this suggests that a temperate terrestrial planet with even modest amounts of N_2 will exhibit rates of lightning production of NO within an order of magnitude of the modern terrestrial rate.

Below, we describe the photochemical models we used to investigate the effect of lightning on the photochemistry of hypothetical abiotic planetary atmospheres, along with the results from those models.

4. Model Description

For this study, we used two one-dimensional, horizontally-averaged photochemical models, which share a common heritage. The model of Harman et al. (2015) is similar to those of Segura et al. (2007) and Tian et al. (2014), and by extension that of Domagal-Goldman et al. (2014), which used the Segura et al. (2007) model with minor modifications. A detailed description of this model can be found in Appendix B of Catling & Kasting (2017). The second model, Atmos, is described in detail in Arney et al. (2016), and while it shares its origins with the Harman et al. model, Zahnle (1986) began significant alterations. These models have differing chemical species, reaction lists, and physics parameterizations, which explains much of the inter-model variability. However, these differences cannot explain the qualitatively different behavior recently reported in the literature, which arises instead from their differing treatments of lightning.

5. Results

To compare with the previous calculations of Domagal-Goldman et al. (2014) and Harman et al. (2015), both the Harman et al. and Atmos models were run without lightning (Figure 2, panels (A) and (C)), while ensuring global redox balance, following Harman et al. We have chosen to highlight both the "worst-case" (highest O_2) scenario of Harman et al. for a terrestrial planet with a 5% CO_2 atmosphere orbiting GJ 876, an M4V star (panels (A) and (B)), as well as for ε Eridani, a K1V star (panels (C) and (D)). These planets

receive ∼60% of the modern Earth's insolation (equivalent to orbiting the Sun at 1.3 au, as described in Harman et al. 2015). However, these results are broadly applicable to all the M dwarf scenarios of Tian et al. (2014), Domagal-Goldman et al. (2014), and Harman et al. (2015), and to the K dwarf scenarios of Domagal-Goldman et al. and Harman et al. The "worst-case" scenario—set to maximize potential abiotic O_2 production—assumes that surface sinks for O_2 are nonexistent, and that CO has an (abiotic) deposition velocity of $10^{-8}\,\mathrm{cm\,s^{-1}}$ (Harman et al. 2015). (The abiotic deposition velocity is derived by assuming that the only sink for CO in solution is hydration to formate.) Both conditions tend to magnify any abiotic O_2 accumulation derived from CO_2 photolysis (Harman et al. 2015). Both the Harman et al. and Atmos models produced atmospheres dominated by CO and O_2 for the M dwarf cases (Figure 2, panel (A)), in line with previous estimates of abiotic O_2 accumulation (Tian et al. 2014; Harman et al. 2015). The Atmos model did not accumulate O_2 in the absence of lightning-produced NO for the K dwarf case (panel (C), dashed curves), which is due to differences in how species like CO_2 and O_3 are treated numerically, as well as differences in model physics.

We then repeated this same calculation with lightning included. The results are shown in Figure 2, panels (B) and (D). In these cases, surface O_2 concentrations are vanishingly small, consistent with estimates for O_2 on the prebiotic Earth and on lifeless planets orbiting F and G stars (Segura et al. 2003; Harman et al. 2015). Similar low-O_2 results are obtained even if the atmospheric CO_2 concentration is increased to as much as 90% by volume.

We conclude that the O_2 false positives reported by Tian et al. (2014) and Harman et al. (2015) would only occur on M-star planets that had no lightning or that had lightning flash rates much lower than that of the modern Earth. Likewise, O_3 would remain low, with O_3 variations between the models used here and in Domagal-Goldman et al. (2014) explained in large part by differences in how global redox balance is ensured, with the remainder of the variation explained by differences in the treatment of CO_2 and O_3 as fixed mixing ratio and long-lived species, respectively. (The methodology of Domagal-Goldman et al. 2014 produced some simulations with anomalous atmospheric redox imbalances, but this overlapped a consistent O_3 build-up in the F star cases—see also Harman et al. 2015.) Because lightning is to be expected on any planet with a wet surface that experiences moist convection (Wong et al. 2017), it seems unlikely that this represents a real false positive. M-star planets may build up high abiotic O_2 levels in other ways (e.g., pre-main sequence water loss), as discussed earlier. But photochemical false positives like those described in Tian et al. (2014) and Harman et al. (2015) are unlikely to actually occur.

6. Discussion

To attempt to quantify how the production of nitrogen oxides by lightning helps to reduce abiotic O_2 concentrations, we have made a list of possible catalytic cycles for recombining CO with O (see Table 1). Our methodology follows that of Stock et al. (2012), who looked at several possible catalytic cycles for the Martian atmosphere. Mars is a reasonable analog for the high-CO_2, low-outgassing planets we have simulated here, except that the Martian atmosphere is much colder and contains much less H_2O.
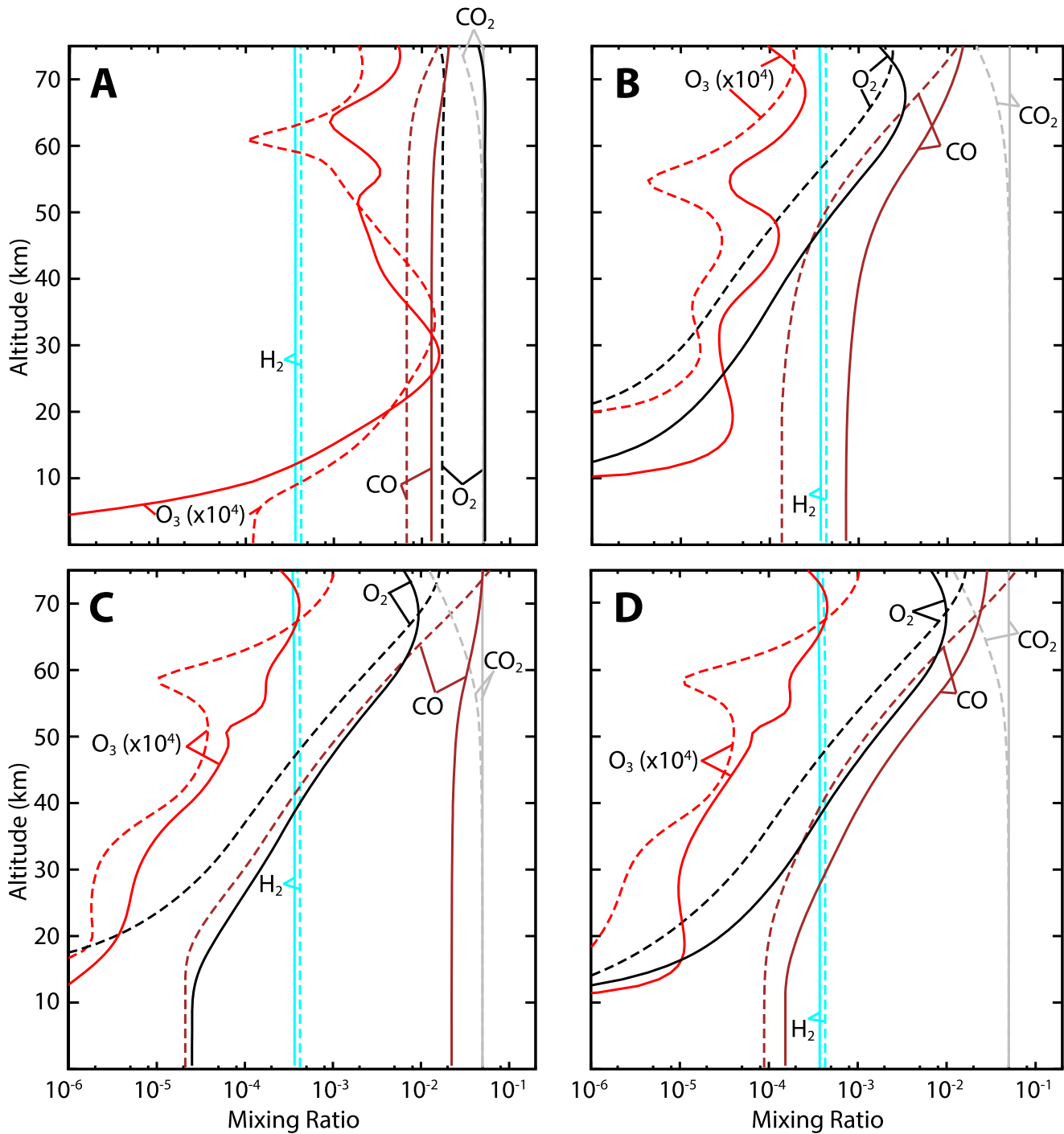
Figure 2. Mixing ratios for the major species in the atmosphere, following Harman et al. (2015). Solid lines are for the model of Harman et al., and dashed lines are for the Atmos model. Each panel is for a 5% CO_2 case for a terrestrial planet orbiting at 1.3 au equivalent around the M star GJ 876 (top panels) and the K star ϵ Eridani (bottom panels). (A), (C) The production of NO by lightning is set to zero; (B), (D) the lightning production of NO is "on," with NO production set by the bulk composition of the atmosphere (Figure 1) and normalized to lightning production in the modern Earth's atmosphere. Again, differences in model specifics (such as the numerical way in which CO_2 and O_3 are treated) yield different results, especially for panel (C) (ϵ Eridani, lightning is set to zero); O_2 and O_3 for all but panel (A) would be very difficult to detect (Domagal-Goldman et al. 2014; Harman et al. 2015).

Several of the catalytic cycles listed share individual chemical reactions between them, but the slow step in each cycle should determine its overall contribution to CO + O recombination (shown as the "net" value below each cycle). In Table 1, we provide side-by-side comparisons of cases for the young Sun, the modern Sun, ϵ Eridani (a K dwarf), and GJ 876 (an M dwarf), based on previous work with false positives (Domagal-Goldman et al. 2014; Tian et al. 2014; Harman et al. 2015) and models for

the spectral evolution of the Sun (Claire et al. 2012). For each star, we have shown a case where lightning is assumed to be producing NO (the "L" columns) and where it is not (the "L-off" columns). In cases where no false positive for O_2 exists, the approximate rate of catalytic destruction of CO and O is equal to or greater than the rate of photolysis of CO_2. For model planets around G-type stars, catalytic destruction of CO and O always outpaces CO_2 photolysis, even with lightning turned off in the model. For K- and M-dwarf

Table 1
Summary of the Major Catalytic Cycles

	2 Gyr Sun		Modern Sun		ϵ Eridani		GJ 876	
	L	L-off	L	L-off	L	L-off	L	L-off
$H_2O + h\nu \rightarrow OH + H$	5.11E10	5.10E10	4.21E10	4.21E10	4.94E9	4.54E9	3.55E8	1.60E8
$CO_2 + h\nu \rightarrow CO + O$	1.77E12	1.77E12	1.39E12	1.39E12	2.37E11	2.38E11	3.29E10	5.16E9
$CO_2 + h\nu \rightarrow CO + O(^1D)$	3.29E11	3.29E11	2.35E11	2.35E11	1.68E12	1.68E12	4.87E11	3.44E11
Cycle 1:								
$O + HO_2 \rightarrow OH + O_2$	1.74E12	1.89E12	1.36E12	1.47E12	1.15E12	8.35E11	1.65E11	2.38E11
$CO + OH \rightarrow CO_2 + H$	2.03E12	2.05E12	1.57E12	1.59E12	1.87E12	1.81E12	4.82E11	3.45E11
$H + O_2 + M \rightarrow HO_2 + M$	2.03E12	2.08E12	1.57E12	1.62E12	2.06E12	1.82E12	4.26E11	3.33E11
Net: $CO + O \rightarrow CO_2$	1.74E12	1.89E12	1.36E12	1.47E12	1.15E12	8.35E11	1.65E11	2.38E11
Cycle 2:								
$H_2O_2 + h\nu \rightarrow OH + OH$	1.42E10	7.43E10	9.19E9	5.15E10	1.70E11	5.35E11	3.87E9	2.79E10
$2(CO + OH \rightarrow CO_2 + H)$	1.02E12	1.02E12	7.85E11	7.93E11	9.36E11	9.07E11	2.41E11	1.73E11
$2(H + O_2 + M \rightarrow HO_2 + M)$	1.02E12	1.04E12	7.84E11	8.07E11	1.03E12	9.10E11	2.13E11	1.67E11
$HO_2 + HO_2 \rightarrow H_2O_2 + O_2$	1.44E10	7.47E10	9.25E9	5.17E10	1.70E11	5.40E11	3.95E9	2.95E10
Net: $2CO + O_2 \rightarrow 2CO_2$	1.42E10	7.43E10	9.19E9	5.15E10	1.70E11	5.35E11	3.87E9	2.79E10
Cycle 3*:								
$NO + HO_2 \rightarrow NO_2 + OH$	2.40E11	0	1.79E11	0	6.03E11	0	3.44E11	0
$CO + OH \rightarrow CO_2 + H$	2.03E12	2.05E12	1.57E12	1.59E12	1.87E12	1.81E12	4.82E11	3.45E11
$H + O_2 + M \rightarrow HO_2 + M$	2.03E12	2.08E12	1.57E12	1.62E12	2.06E12	1.82E12	4.26E11	3.33E11
$NO_2 + h\nu \rightarrow NO + O$	1.89E11	0	1.67E11	0	4.74E11	0	2.02E11	0
$O + O + M \rightarrow O_2 + M$	2.09E11	2.08E11	1.36E11	1.35E11	2.43E11	2.60E11	1.98E11	1.16E11
Net: $CO + O \rightarrow CO_2$	1.89E11	0	1.36E11	0	2.43E11	0	1.98E11	0
Cycle 4:								
$O + NO_2 \rightarrow NO + O_2$	1.41E11	0	1.02E11	0	1.28E11	0	1.34E11	0
$NO + HO_2 \rightarrow NO_2 + OH$	2.40E11	0	1.79E11	0	6.03E11	0	3.44E11	0
$CO + OH \rightarrow CO_2 + H$	2.03E12	2.05E12	1.57E12	1.59E12	1.87E12	1.81E12	4.82E11	3.45E11
$H + O_2 + M \rightarrow HO_2 + M$	2.03E12	2.08E12	1.57E12	1.62E12	2.06E12	1.82E12	4.26E11	3.33E11
Net: $CO + O \rightarrow CO_2$	1.41E11	0	1.02E11	0	1.28E11	0	1.34E11	0
Cycle 5:								
$NO + HO_2 \rightarrow NO_2 + OH$	2.40E11	0	1.79E11	0	6.03E11	0	3.44E11	0
$NO_2 + h\nu \rightarrow NO + O$	1.89E11	0	1.67E11	0	4.74E11	0	2.02E11	0
$O + HO_2 \rightarrow OH + O_2$	1.74E12	1.89E12	1.36E12	1.47E12	1.15E12	8.35E11	1.65E11	2.38E11
$2(CO + OH \rightarrow CO_2 + H)$	1.02E12	1.02E12	7.85E11	7.93E11	9.36E11	9.07E11	2.41E11	1.73E11
$2(H + O_2 + M \rightarrow HO_2 + M)$	1.02E12	1.04E12	7.84E11	8.07E11	1.03E12	9.10E11	2.13E11	1.67E11
Net: $2CO + O_2 \rightarrow 2CO_2$	1.89E11	0	1.67E11	0	4.74E11	0	1.65E11	0
Total H_xO_y catalysis (1 and 2)	1.76E12	1.96E12	1.36E12	1.52E12	1.32E12	1.37E12	1.69E11	2.66E11
Total NO_x catalysis (3–5)	5.18E11	0	4.04E11	0	8.49E11	0	4.97E11	0
Total catalysis:	2.28E12	1.96E12	1.77E12	1.52E12	2.17E12	1.37E12	6.66E11	2.66E11
Total CO_2 photolysis:	2.10E12	2.09E12	1.63E12	1.63E12	1.91E12	1.92E12	5.20E11	3.50E11
Ground-level O_2 mixing ratio	2.1E-14	9.1E-19	2.3E-14	6.5E-19	7.5E-14	2.6E-5	6.9E-13	5.20E-2
Ground-level CO mixing ratio	1.4E-5	1.4E-5	1.4E-5	1.4E-5	1.5E-4	2.2E-2	7.20E-4	1.30E-2

Note. Summary of the major catalytic cycles suggested by Stock et al. (2012) occurring in the Martian atmosphere. Each value is the column-integrated rate ($cm^{-2}\,s^{-1}$) for the reaction listed, except the mixing ratios. This is an analog for the 5% CO_2, low instellation (1.3 au equivalent), low volcanic outgassing atmospheres shown here and in Harman et al. (2015). First column, cycles 1–5; note that we have modified cycle 3.

planets, O_2 concentrations remain low only if there are additional nitrogen–oxide-based catalytic cycles, besides those initiated by photolysis of H_2O. In other words, in our simulations of these worlds, O_2 does not accumulate if lightning is included in the model, consistent with the results of Domagal-Goldman et al. (2014). But CO_2 photolysis outpaces water vapor for the K- and M-dwarf no-lightning ("L-off") cases, leading to atmospheric O_2 accumulation in these simulations, consistent with Tian et al. (2014) and Harman et al. (2015).

Importantly, there is an overlap between where N_2-derived NO may be sufficient to drive the recombination of CO and O_2, and where N_2 is undetectable. Below approximately 0.5 bar N_2, the N_2 dimer feature would be largely undetectable (Schwieterman et al. 2015), but the NO production rate would still be large enough to catalytically recombine O_2 with CO, as long as pN_2 is greater than $\sim$0.01 bar. However, the lower limit for pN_2 $\sim$0.08 bar would be set by temperate water loss and O_2 accumulation (Wordsworth & Pierrehumbert 2014). For 0.5 bar $< pN_2 < \sim$0.08 bar, then,

separating these two false positives using the N_2 dimer alone is not possible, and additional constraints on the atmospheric composition or total pressure would be needed. Secondary features such as the absence of the O_2 dimer would rule out $O_2 > 0.5$ bar (Misra et al. 2014), and high signal-to-noise measurements of several spectral features may place a useful lower limit on total atmospheric pressure (Des Marais et al. 2002; Misra et al. 2014), although these types of observations would be difficult with the *JWST* (Batalha et al. 2018). Additional information from Rayleigh scattering (e.g., Selsis 2004; Benneke & Seager 2012) or thermal phase curves (e.g., Koll & Abbot 2015) could also be used to constrain atmospheric pressure.

6.1. Additional Sinks for Abiotic Oxygen

In addition to the catalytic recombination of CO and O_2 by NO, other geological sinks for abiotic O_2 exist on Earth-like planets. Plate tectonics exposes new material that would chemically react with free oxygen, but whether and under what circumstances plate tectonics started on Earth (e.g., Condie & Pease 2008; Korenaga 2013), let alone on other planets (e.g., Valencia et al. 2007; Korenaga 2010; van Summeren et al. 2011; van Heck & Tackley 2011; Foley et al. 2012; Noack & Breuer 2014), remains uncertain (and potentially unanswerable; see Lenardic & Crowley 2012). Oxidative weathering may be relatively insensitive to the exposed land fraction, if it behaves similarly to silicate weathering (Abbot et al. 2012). In the absence of plate tectonics, however, the addition of reducing gases from the interior of the planet would act as a sink for O_2. Volcanic outgassing is tangentially related to the tectonic activity of a planet, both being driven principally by internal heating (from planetary formation and radioactive decay). However, the radionuclide budget of a planet is expected to decrease with time, but also as a function of its formation age (Gonzalez et al. 2001). The composition and flux of volcanic gases is also incredibly complex, depending on redox state of the mantle (Kasting et al. 1993a), the source material (Schaefer & Fegley 2007), and the volcanic setting (e.g., Burgisser & Scaillet 2007; Gaillard et al. 2011; Gaillard & Scaillet 2014), but may remain consistent over the lifetime of the planet (e.g., Trail et al. 2011). All three terrestrial planets in our solar system demonstrate varying amounts of volcanic activity (e.g., Smrekar et al. 2010; Hauber et al. 2011), despite their divergent evolutionary paths.

6.2. Other Considerations

Smaller amounts of lightning-produced NO, consistent with suggestions for ocean worlds (Hodosán et al. 2016), can still be effective in limiting abiotic O_2 buildup. Even if the rate of NO production is decreased by an order of magnitude, O_2 concentrations in our "worst case" GJ 876 scenario remain at or below ∼1 ppb at the surface. However, NO production rates more than 30 times less than modern are insufficient to prevent significant accumulations of O_2 in our 5% CO_2 GJ 876 case. That said, the models used here have parameterized lightning production of NO based on the modern Earth, which would underestimate lightning occurrence (and thus NO production) for warmer, wetter atmospheres (e.g., Wong et al. 2017).

In our model, lightning is assumed to be the only source of NO. However, other sources of NO exist, and NO is not the only catalyst capable of recombining CO and O_2. Volcanoes are a known source of NO (e.g., von Glasow et al. 2009), and could have introduced fluxes of NO into the early Earth's

atmosphere comparable to that produced by lightning fixation of NO on the modern Earth (Martin et al. 2007). GCRs and coronal mass ejections (CME) can also produce nitric oxides in the atmosphere (e.g., Nicolet 1975; Scalo et al. 2007; Airapetian et al. 2016). Planets orbiting M dwarfs experience larger and more frequent flares (e.g., Airapetian et al. 2017) and enhanced GCR fluxes due to the proximity of a planet in the habitable zone to its host star (e.g., Grenfell et al. 2007), suggesting that the NO production estimates outlined below are conservative. Chlorine and bromine radicals could potentially operate in the same way as NO (even interacting with NO_x, which further complicates the story). These radicals can be derived from sea salt spray (Finlayson-Pitts 2003), and are relevant to the O_2 and O_3 chemistry on Venus (e.g., Mills et al. 2006). Further work could quantify the effects of these species on abiotic O_2 concentrations in more Earth-like atmospheres.

As always, constraints on the atmospheric composition of an exoplanet will be invaluable in determining whether an O_2 absorption signal is really an indicator of life. Substantial concentrations of CH_4, or of H_2O, N_2, CO_2, and CO, combined with the absence of a substantial O_2 dimer spectral feature (indicative of a post-runaway greenhouse atmosphere), would effectively exclude all known false positive mechanisms (Schwieterman et al. 2016; Wang et al. 2016). Several methods along these lines meant to minimize false positives have been proposed (e.g., Desch et al. 2018; Harman & Domagal-Goldman 2018). This work suggests that, even in the absence of such constraints, the simultaneous detection of $O_2 + H_2O + N_2$ would be strongly suggestive of the presence of life on a terrestrial exoplanet orbiting in the habitable zone.

7. Conclusion

In the cases outlined here, lightning eliminates the reported photochemical O_2 false positives in the atmospheres of terrestrial planets around small stars. We conclude that: (1) a self-consistent habitable (but lifeless) terrestrial planet is likely to have several mechanisms at work that reduce photolysis-driven disequilibrium, including lightning and outgassing of reduced gases, and (2) physical processes beyond the scope of gas-phase chemistry *control* the chemical composition of a planet's atmosphere. On Earth, biology is the dominant control. For lifeless worlds, these controls include boundary conditions reflecting the assumed chemistry of the ocean, and phenomena like lightning, as we have shown here. Modelers must weigh the potential impact of these secondary processes and reservoirs and work to connect assumptions to geologically plausible scenarios. The production of NO is not limited to lightning, however, and M-dwarf host stars, with their myriad other complications, have several substantial alternative NO production routes. Consequently, the presence of O_2, alongside reasonable concentrations of H_2O, CO_2, and N_2, should be regarded as a robust biosignature of terrestrial exoplanets orbiting within habitable zones. Future plans to explore the influence of lightning on atmospheric composition will couple photochemical and climate simulations to better capture the interaction of lightning occurrence and O_2 accumulations.

ORCID iDs

C. E. Harman ⓘ https://orcid.org/0000-0003-2281-1990
S. D. Domagal-Goldman ⓘ https://orcid.org/0000-0003-0354-9325
F. Tian ⓘ https://orcid.org/0000-0002-9607-560X
J. F. Kasting ⓘ https://orcid.org/0000-0003-4042-2067

References

Abbot, D. S., Cowan, N. B., & Ciesla, F. J. 2012, ApJ, 756, 178
Airapetian, V. S., Glocer, A., Gronoff, G., Hébrard, E., & Danchi, W. 2016, NatGe, 9, 452
Airapetian, V. S., Glocer, A., Khazanov, G. V., et al. 2017, ApJL, 836, L3
Arney, G., Domagal-Goldman, S. D., Meadows, V. S., et al. 2016, AsBio, 16, 873
Batalha, N. E., Lewis, N. K., Line, M. R., Valenti, J., & Stevenson, K. 2018, ApJL, 856, L34
Benneke, B., & Seager, S. 2012, ApJ, 753, 100
Berner, R. A., & Canfield, D. E. 1989, AmJS, 289, 333
Burgisser, A., & Scaillet, B. 2007, Natur, 445, 194
Catling, D., & Kasting, J. F. 2017, Atmospheric Evolution on Inhabited and Lifeless Worlds (Cambridge: Cambridge Univ. Press)
Chameides, W. L. 1978, GeoRL, 5, 17
Chameides, W. L., & Walker, J. C. 1981, OLEB, 11, 291
Claire, M. W., Sheets, J., Cohen, M., et al. 2012, ApJ, 757, 95
Condie, K. C., & Pease, V. (ed.) 2008, When did Plate Tectonics Begin on Planet Earth?, Vol. 440 (Boulder, CO: GSA)
Desch, S. J., Kane, S., Lisse, C. M., et al. 2018, arXiv:1801.06935
Des Marais, D. J., Harwit, M. O., Jucks, K. W., et al. 2002, AsBio, 2, 153
Domagal-Goldman, S. D., Segura, A., Claire, M. W., Robinson, T. D., & Meadows, V. S. 2014, ApJ, 792, 90
Finlayson-Pitts, B. J. 2003, ChRv, 103, 4801
Foley, B. J., Bercovici, D., & Landuyt, W. 2012, E&PSL, 331, 281
Gaillard, F., & Scaillet, B. 2014, E&PSL, 403, 307
Gaillard, F., Scaillet, B., & Arndt, N. T. 2011, Natur, 478, 229
Gao, P., Hu, R., Robinson, T. D., Li, C., & Yung, Y. L. 2015, ApJ, 806, 249
Gonzalez, G., Brownlee, D., & Ward, P. 2001, Icar, 152, 185
Grenfell, J. L., Grießmeier, J. M., Patzer, B., et al. 2007, AsBio, 7, 208
Harman, C. E., & Domagal-Goldman, S. D. 2018, in Handbook of Exoplanets, ed. H. J. Deeg & J. A. Belmonte (Cham: Springer), 1
Harman, C. E., Schwieterman, E. W., Schottelkotte, J. C., & Kasting, J. F. 2015, ApJ, 812, 137
Hauber, E., Brož, P., Jagert, F., Jodłowski, P., & Platz, T. 2011, GeoRL, 38, L10201
Hodosán, G., Helling, C., Asensio-Torres, R., Vorgul, I., & Rimmer, P. B. 2016, MNRAS, 461, 3927
Hu, R., Seager, S., & Bains, W. 2012, ApJ, 761, 166
Kane, S. R., Kopparapu, R. K., & Domagal-Goldman, S. D. 2014, ApJL, 794, L5
Kasting, J. F. 1979, PhD Dissertation, Univ. Michigan
Kasting, J. F. 1988, Icar, 74, 472
Kasting, J. F. 1990, OLEB, 20, 199
Kasting, J. F., Eggler, D. H., & Raeburn, S. P. 1993a, JG, 101, 245
Kasting, J. F., Whitmire, D. P., & Reynolds, R. T. 1993b, Icar, 101, 108
Kiang, N. Y., Siefert, J., & Blankenship, R. E. 2007, AsBio, 7, 222
Koll, D. D., & Abbot, D. S. 2015, ApJ, 802, 21
Kopparapu, R. K., Ramirez, R., Kasting, J. F., et al. 2013, ApJ, 765, 131

Korenaga, J. 2010, ApJL, 725, L43
Korenaga, J. 2013, AREPS, 41, 117
Kump, L. R. 2008, Natur, 451, 277
Léger, A., Fontecave, M., Labeyrie, A., et al. 2011, AsBio, 11, 335
Lenardic, A., & Crowley, J. W. 2012, ApJ, 755, 132
Lenton, T. M. 2001, GCBio, 7, 613
Luger, R., & Barnes, R. 2015, AsBio, 15, 119
Lyons, T. W., Reinhard, C. T., & Planavsky, N. J. 2014, Natur, 506, 307
Martin, R. S., Mather, T. A., & Pyle, D. M. 2007, GeCoA, 71, 3673
Meadows, V. S. 2017, AsBio, 17, 1022
Meadows, V. S., Reinhard, C. T., Arney, G. N., et al. 2017, arXiv:1705.07560
Miles, B. E., & Shkolnik, E. L. 2017, arXiv:1705.03583
Mills, F. P., Sundaram, M., Slanger, T. G., Allen, M., & Yung, Y. L. 2006, AdG, 3, 109
Misra, A., Meadows, V., Claire, M., & Crisp, D. 2014, AsBio, 14, 67
Navarro-Gonzalez, R., McKay, C. P., & Mvondo, D. N. 2001, Natur, 412, 61
Nicolet, M. 1975, P&SS, 23, 637
Nna Mvondo, D., Navarro-González, R., McKay, C. P., Coll, P., & Raulin, F. 2001, AdSpR, 27, 217
Noack, L., & Breuer, D. 2014, P&SS, 98, 41
Planavsky, N. J., Reinhard, C. T., Wang, X., et al. 2014, Sci, 346, 635
Ramirez, R. M., & Kaltenegger, L. 2014, ApJL, 797, L25
Rimmer, P. B., & Helling, C. 2016, ApJS, 224, 9
Scalo, J., Kaltenegger, L., Segura, A., et al. 2007, AsBio, 7, 85
Schaefer, L., & Fegley, B., Jr 2007, Icar, 186, 462
Schumann, U., & Huntrieser, H. 2007, ACP, 7, 3823
Schwieterman, E. W., Meadows, V. S., Domagal-Goldman, S. D., et al. 2016, ApJL, 819, L13
Schwieterman, E. W., Robinson, T. D., Meadows, V. S., Misra, A., & Domagal-Goldman, S. 2015, ApJ, 810, 57
Seager, S., Bains, W., & Hu, R. 2013, ApJ, 775, 104
Segura, A., Krelove, K., Kasting, J. F., et al. 2003, AsBio, 3, 689
Segura, A., Meadows, V. S., Kasting, J. F., Crisp, D., & Cohen, M. 2007, A&A, 472, 665
Selsis, F. 2004, in ASP Conf. Proc., Vol. 321, Extrasolar Planets: Today and Tomorrow, ed. J.-P. Beaulie et al. (San Francisco, CA: ASP), 170
Smrekar, S. E., Stofan, E. R., Mueller, N., et al. 2010, Sci, 328, 605
Som, S. M., Buick, R., Hagadorn, J. W., et al. 2016, NatGe, 9, 448
Som, S. M., Catling, D. C., Harnmeijer, J. P., Polivka, P. M., & Buick, R. 2012, Natur, 484, 359
Stock, J. W., Grenfell, J. L., Lehmann, R., Patzer, A. B. C., & Rauer, H. 2012, P&SS, 68, 18
Stozhkov, Y. I. 2003, JPhG, 29, 913
Tian, F. 2015, E&PSL, 432, 126
Tian, F., France, K., Linsky, J. L., Mauas, P. J., & Vieytes, M. C. 2014, E&PSL, 385, 22
Trail, D., Watson, E. B., & Tailby, N. D. 2011, Natur, 480, 79
Valencia, D., O'connell, R. J., & Sasselov, D. D. 2007, ApJL, 670, L45
van Heck, H. J., & Tackley, P. J. 2011, E&PSL, 310, 252
van Summeren, J., Conrad, C. P., & Gaidos, E. 2011, ApJL, 736, L15
von Glasow, R., Bobrowski, N., & Kern, C. 2009, ChGeo, 263, 131
Wallace, M. W., Hood, A. V. S., Shuster, A., et al. 2017, E&PSL, 466, 12
Wang, Y., Tian, F., Li, T., & Hu, Y. 2016, Icar, 266, 15
Way, M. J., Del Genio, A. D., Kiang, N. Y., et al. 2016, GeoRL, 43, 8376
Williams, E., & Stanfill, S. 2002, CRPhy, 3, 1277
Wong, M. L., Charnay, B. D., Gao, P., Yung, Y. L., & Russell, M. J. 2017, AsBio, 17, 975
Wordsworth, R., & Pierrehumbert, R. 2014, ApJL, 785, L20
Wordsworth, R. D., Schaefer, L. K., & Fischer, R. A. 2018, AJ, 155, 195
Zahnle, K. J. 1986, JGRD, 91, 2819